Extremal Trajectories for
Bounded Velocity Differential Drive Robots

Devin J. Balkcom   Matthew T. Mason

Robotics Institute and Computer Science Department
Carnegie Mellon University
Pittsburgh PA 15213

Abstract

This paper applies Pontryagin's Maximum Principle to the time optimal control of differential drive mobile robots with velocity bounds. The Maximum Principle gives necessary conditions for time optimality. Extremal trajectories are those which satisfy these conditions, and are thus a superset of the time optimal trajectories. This paper derives a compact geometrical structure for extremal trajectories and shows that extremal trajectories are always composed of rotations about the robot center and straight line motions. Further necessary conditions are obtained.

1 Introduction

This paper focuses on the application of Pontryagin's Maximum Principle to the time optimal control of diff drive mobile robots with velocity bounds. A *diff drive* robot has two independently driven coaxial wheels. By *velocity bounds,* we mean that the wheel velocities are bounded, but there are no bounds on wheel acceleration. In fact, discontinuities in wheel velocity are allowed.

Pontryagin's Maximum Principle yields conditions that are necessary but not sufficient for time optimal trajectories. Hence the trajectories that satisfy the Maximum Principle are called *extremal* trajectories, and are a superset of the time optimal trajectories. The Maximum Principle provides a compact geometrical description of the extremal trajectories, and thus gives us a tool for enumerating and exploring time optimal trajectories. Figure 1 shows two of the six different extremal types.

1.1 Previous Work

We know of no previous work on time-optimal control of the bounded velocity diff drive robot, but the techniques employed here draw extensively on the techniques devel-
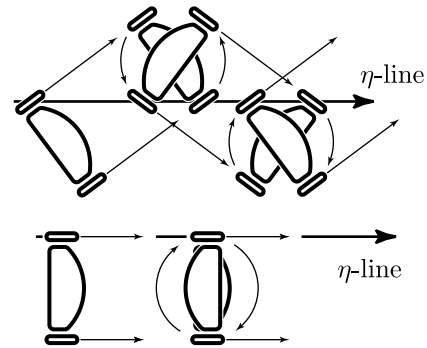

Figure 1: Two extremals: *zigzag right* and *tangent CW*. Other extremal types are *zigzag left*, *tangent CCW*, and turning in place: *CW* and *CCW*. Straight lines are special cases of zigzags or tangents.

oped for steered vehicles [6, 2, 5, 4]. Interested readers should see our companion paper [1] for a broader discussion.

2 Assumptions, definitions, notation

The state of the robot is $q = (x, y, \theta)$, where the robot reference point (x, y) is centered between the wheels, and the robot direction θ is 0 when the robot is facing along the x-axis, and increases in the counterclockwise direction (Figure 2). The robot's velocity in the forward direction is v and its angular velocity is ω. The robot's width is $2b$. The wheel angular velocities are ω_l and ω_r. With a suitable choice of units we obtain

$$v = \frac{1}{2}(\omega_l + \omega_r) \tag{1}$$
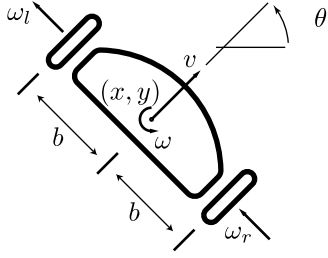
$$\omega = \frac{1}{2b}(\omega_r - \omega_l) \tag{2}$$

Figure 2: Notation

Figure 3: Bounds on (ω_l, ω_r)

and

$$\omega_l = v - b\omega \tag{3}$$

$$\omega_r = v + b\omega \tag{4}$$

The robot is a system with control input $w(t) = (\omega_l(t), \omega_r(t))$ and output $q(t)$. Admissible controls are bounded Lebesgue measurable functions from time interval $[0, T]$ to the closed box $W = [-1, 1] \times [-1, 1]$, where T is the time at which the robot reaches the goal. (see Figure 3).

It follows immediately that $v(t)$ and $\omega(t)$ are measurable functions defined on the same interval. Given initial conditions $q_s = (x_s, y_s, \theta_s)$ the path of the robot is given by

$$\theta(t) = \theta_s + \int_0^t \omega \tag{5}$$

$$x(t) = x_s + \int_0^t v \cos(\theta) \tag{6}$$

$$y(t) = y_s + \int_0^t v \sin(\theta) \tag{7}$$

It follows that θ, x, y are continuous, that their time derivatives exist almost everywhere, and that

$$\dot{\theta} = \omega \quad \text{a.e.} \tag{8}$$

$$\dot{x} = v \cos(\theta) \quad \text{a.e.} \tag{9}$$

$$\dot{y} = v \sin(\theta) \quad \text{a.e.} \tag{10}$$

We also define rectified path length in the plane of robot positions

$$s(t) = \int_0^t |v| \tag{11}$$

and in the circle of robot orientations

$$\sigma(t) = \int_0^t |\omega| \tag{12}$$

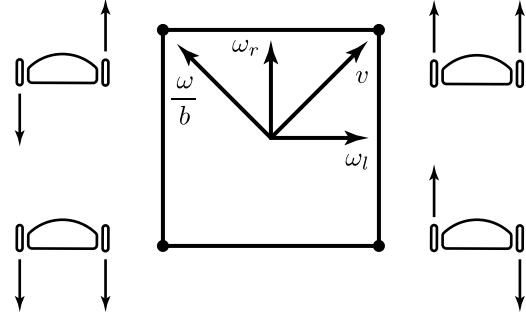We also need a notation for trajectories. Later sections show that extremal trajectories are composed of straight lines and turns about the robot's center. We will represent *forward* by ⇑, *backward* by ⇓, *left turn* by ↶, and *right turn* by ↷. Thus the trajectory ↶⇑↶ can be read "left forward left". When necessary, a subscript will indicate the distance or angle traveled.

3 Controllability

Before applying Pontryagin's Maximum Principle to derive necessary conditions on optimal trajectories, we must show that trajectories exist for any given pair of start and goal states (controllability) and then that time optimal trajectories exist for any given pair of start and goal states.

To prove controllability we combine equations 1, 2, 8, 9, and 10 to obtain

$$\begin{pmatrix} \dot{x} \\ \dot{y} \\ \dot{\theta} \end{pmatrix} = \omega_l f_l + \omega_r f_r \tag{13}$$

where f_l and f_r are the vector fields corresponding to the left and right wheels:

$$f_l = \begin{pmatrix} \frac{1}{2}\cos\theta \\ \frac{1}{2}\sin\theta \\ -\frac{1}{2b} \end{pmatrix} \tag{14}$$

$$f_r = \begin{pmatrix} \frac{1}{2}\cos\theta \\ \frac{1}{2}\sin\theta \\ \frac{1}{2b} \end{pmatrix} \tag{15}$$

Vector field f_l corresponds to turning about a center located under the right wheel, and f_r corresponds to turning about a center located under the left wheel.

We construct a third vector field which is the Lie bracket of f_l and f_r:

$$f_{Lie} = [f_l, f_r] = Df_r\, f_l - Df_l\, f_r \tag{16}$$

where Df is the Jacobian matrix, obtained by taking partials of the field f with respect to the three state variables.

Expanding these Jacobians and simplifying:

$$f_{Lie} = \begin{pmatrix} \frac{1}{2b} \sin \theta \\ -\frac{1}{2b} \cos \theta \\ 0 \end{pmatrix} \qquad (17)$$

This third vector field corresponds to an infinitesimal parallel parking maneuver of the robot, translating the robot to its right. For nonzero b it is readily observed that the three vector fields are linearly independent, satisfying the Lie Algebra Rank Condition. The diff drive robot is also symmetric, meaning that an admissible trajectory with time reversed yields an admissible trajectory. It follows from Theorem 2 of Sussman and Tang [6] that the bounded velocity diff drive robot is globally controllable, *i.e.* that admissible trajectories exist for every pair of start and goal configurations.

4 Existence of optimal trajectories.

Theorem 1 *For any given start and goal configuration of a bounded velocity diff drive in the plane without obstacles, there is a time optimal control.*

Proof: Theorem 6 of Sussman and Tang [6] gives conditions sufficient for the existence of time optimal controls. For our case the conditions are:

- the system state variable $q = (x, y, \theta)$ takes values in an open subset of a differentiable manifold;

- the vector fields f_l and f_r are locally Lipschitz;

- the input $w = (\omega_l, \omega_r)$ takes values in a compact convex subset of R^2;

- the admissible controls are measurable functions on compact subintervals of R;

- *completeness:* for every start state and every control over some time interval, there is a trajectory starting at the start state, and defined over the whole interval.

The conditions are readily verified for the bounded velocity diff drive, and we know from Section 3 that trajectories exist for every pair of given start and goal states. It follows that time optimal controls exist for every given start and goal state. □

5 Pontryagin's Maximum Principle. Extremal controls.

This section uses Pontryagin's Maximum Principle [3] to derive necessary conditions for time optimal trajectories of the bounded velocity diff drive robot. The robot system is described by

$$\dot{q} = \begin{pmatrix} \dot{x} \\ \dot{y} \\ \dot{\theta} \end{pmatrix} = \begin{pmatrix} \frac{1}{2}(\omega_l + \omega_r)\cos(\theta) \\ \frac{1}{2}(\omega_l + \omega_r)\sin(\theta) \\ \frac{1}{2b}(\omega_r - \omega_l) \end{pmatrix} \qquad (18)$$

where our input is

$$w = \begin{pmatrix} \omega_l \\ \omega_r \end{pmatrix} \in W$$

Define λ to be an R^3-valued function of time called the *adjoint vector*:

$$\lambda(t) = \begin{pmatrix} \lambda_1(t) \\ \lambda_2(t) \\ \lambda_3(t) \end{pmatrix}$$

Let $H : R^3 \times SE^2 \times W \to R$ be the *Hamiltonian*:

$$H(\lambda, q, w) = < \lambda, \omega_l f_l + \omega_r f_r >$$

where f_l and f_r are the vector fields defined by equations 14 and 15.

The maximum principle states that for a control $w(t)$ to be optimal, it is *necessary* that there exist a nontrivial (not identically zero) adjoint vector $\lambda(t)$ satisfying the *adjoint equation*:

$$\dot{\lambda} = -\frac{\partial}{\partial q} H \qquad (19)$$

while the control $w(t)$ minimizes the Hamiltonian at all t:

$$H(\lambda, q, w) = \min_{z \in W} H(\lambda, q, z) = \lambda_0. \qquad (20)$$

with $\lambda_0 \geq 0$. Equation 19 is called the *adjoint equation* and equation 20 is called the *minimization equation*.

For the bounded velocity diff drive, the adjoint equation gives

$$\dot{\lambda} = \frac{\omega_l + \omega_r}{2} \begin{pmatrix} 0 \\ 0 \\ \lambda_1 \sin \theta - \lambda_2 \cos \theta \end{pmatrix} \qquad (21)$$

Fortunately these equations can be integrated to obtain an expression for the adjoint vector. First we observe that λ_1 and λ_2 are constant and define c_1 and c_2 accordingly

$$\lambda_1(t) = c_1 \qquad (22)$$
$$\lambda_2(t) = c_2 \qquad (23)$$

For λ_3 we have the equation

$$\dot{\lambda}_3 = \frac{\omega_l + \omega_r}{2}(\lambda_1 \sin \theta - \lambda_2 \cos \theta) \qquad (24)$$

But we can substitute from equations 1, 9, and 10 to obtain

$$\dot{\lambda}_3 = c_1 \dot{y} - c_2 \dot{x} \tag{25}$$

which is integrated to obtain the solution for λ_3:

$$\lambda_3 = c_1 y - c_2 x + c_3 \tag{26}$$

where c_3 is our third and final integration constant. It will be convenient in the rest of the paper to define a function η of x and y:

$$\eta(x, y) = c_1 y - c_2 x + c_3 \tag{27}$$

So then the adjoint equation is satisfied by

$$\lambda = \begin{pmatrix} c_1 \\ c_2 \\ \eta(x, y) \end{pmatrix} \tag{28}$$

for any c_1, c_2, c_3 not all equal to zero.

Let the η-*line* be the line of points (x, y) satisfying $\eta(x, y) = 0$, and note that $\eta(x, y)$ gives a scaled directed distance of a point (x, y) from the η-line. Let the *right half plane* be the points satisfying

$$\eta(x, y) > 0 \tag{29}$$

and let the *left half plane* be the points satisfying

$$\eta(x, y) < 0 \tag{30}$$

We also define a direction for the η-line consistent with our the choice of "left" and "right" for the half planes.

The minimization equation 20 can be rewritten

$$\omega_l \phi_l + \omega_r \phi_r = \min_{z_l, z_r} z_l \phi_l + z_r \phi_r \tag{31}$$

where ϕ_l and ϕ_r are defined to be the two *switching functions*:

$$\phi_l = \ <\lambda, f_l> \tag{32}$$

$$= \ -\frac{1}{2b} \eta(x + b \sin \theta, y - b \cos \theta) \tag{33}$$

$$\phi_r = \ <\lambda, f_r> \tag{34}$$

$$= \ \frac{1}{2b} \eta(x - b \sin \theta, y + b \cos \theta) \tag{35}$$

Note that the wheels' coordinates can be written

$$\begin{pmatrix} x_l \\ y_l \end{pmatrix} = \begin{pmatrix} x - b \sin \theta \\ y + b \cos \theta \end{pmatrix} \tag{36}$$

$$\begin{pmatrix} x_r \\ y_r \end{pmatrix} = \begin{pmatrix} x + b \sin \theta \\ y - b \cos \theta \end{pmatrix} \tag{37}$$

so the switching functions can be written

$$\phi_l = \ -\frac{1}{2b} \eta(x_r, y_r) \tag{38}$$

$$\phi_r = \ \frac{1}{2b} \eta(x_l, y_l) \tag{39}$$

Now the minimization equation says that if the controls ω_l, ω_r are optimal then they minimize the Hamiltonian $H = \omega_l \phi_l + \omega_r \phi_r$. Note that $\eta(x_r, y_r)$ and $\eta(x_l, y_l)$ are the location of the left and right wheels relative to the η-line. (e.g, if $\eta(x_r, y_r) > 0$, then the right wheel is the right half plane.) This implies the optimal controls can be expressed

$$\omega_l \begin{cases} = 1 & \text{if right wheel} \in \text{right half plane} \\ \in [-1, 1] & \text{if right wheel} \in \eta\text{-line} \\ = -1 & \text{if right wheel} \in \text{left half plane} \end{cases} \tag{40}$$

$$\omega_r \begin{cases} = 1 & \text{if left wheel} \in \text{left half plane} \\ \in [-1, 1] & \text{if left wheel} \in \eta\text{-line} \\ = -1 & \text{if left wheel} \in \text{right half plane} \end{cases} \tag{41}$$

If $c_1 = c_2 = 0$, then the η-line is at infinity, and the entire plane is the left half plane or the right half plane, depending on the sign of c_3. (Recall that all three integration constants cannot be simultaneously zero.)

The location of the η-line depends on the apparently arbitrary integration constants. The maximum principle does not give the location of the line; it merely says that if we have an optimal control then the line exists and the optimal control must conform to the equations above. The question that naturally arises is how to locate the line properly, given the start and goal configurations of the robot. There seems to be no direct way of doing so. Rather, we must use other means to identify the extremal trajectory.

The behavior of the robot falls into one of the following cases (Figure 1):

- CCW and CW: If the robot is in the left half plane and out of reach of the η-line, it turns in the counterclockwise direction (CCW). CW is similar.

- TCCW and TCW (Tangent CCW and Tangent CW). If the robot is in the left half plane, but close enough that a circumscribed circle is tangent to the η-line, then the robot may either roll straight along the line, or it may turn through any positive multiple of π. TCW is similar.

- ZR and ZL: If the circumscribed circle crosses the η-line, then a zigzag behavior occurs. The robot rolls straight in the η-line's direction until one wheel crosses. It then turns until the other wheel crosses, and then goes straight again. There are two non-degenerate patterns: ... ⇑⌒⇓⌒ ... called *zigzag right* ZR, and ... ⇑⌒⇓⌒ ... called *zigzag left* ZL.

Examining these classes, we see that

Theorem 2 *For an optimal trajectory,*

$$t = s(t) + b\sigma(t) \tag{42}$$

Proof: Extremal trajectories are composed only of turns and straight lines.□

Note that in [1], we demonstrate that equation 42 actually holds for any trajectory such that $\max(|\omega_l|, |\omega_r|) = 1$ for almost all t; i.e., for trajectories in which one control is always saturated. This may provide some intuition for why turns and straights are faster than curves.

6 Further necessary conditions for optimality.

Every nontrivial time-optimal control must fall in one of the above cases. However, the converse is definitely not true—not every trajectory conforming to the cases above is optimal. For example, a robot turning in place for several revolutions is not time optimal. To keep the distinction clear, we refer to trajectories satisfying Pontryagin's Maximum Principle as *extremal*, and we note that the time-optimal trajectories are a subset of the extremal trajectories.

We place a coordinate system as follows. Put the robot start on the negative x axis, and the put the goal on the positive x axis, such that $x_s = -x_g$. The y axis is then the perpendicuar bisector of the segment between x_s and x_g, oriented in the usual way. We define the range of θ_s and θ_g to be $(-\pi, \pi]$.

Restrictions on TCCW and TCW trajectories

Theorem 3 *The cost of the fastest* TCW *or* TCCW *trajectory is*

$$t = b(\min(|\theta_s| + |\theta_g|, 2\pi - |\theta_s| - |\theta_g|)) + (x_g - x_s) \tag{43}$$

Furthermore, optimal trajectories of type TCW *or* TCCW *can be composed of no more than three actions.*

Proof: TCW or TCCW trajectories with three actions are of the form straight-turn$_{\pi(2n+1)}$-straight or of the form turn-straight-turn. The theorem is elementary for the first case.

Now consider turn-straight-turn trajectories. If we let ϕ_1 and ϕ_2 be the magnitudes of the first and second turns respectively, the cost of this trajectory is
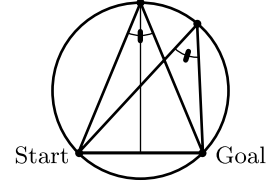
$$t = b(\phi_1 + \phi_2) + (x_g - x_s) \tag{44}$$

Figure 4: Zigzags of three turns are not optimal

Choosing turning directions to minimize equation 44, we find that $|\theta_s| + |\theta_g|$ is the magnitude of the total angle turned through by the fastest turn-⇑-turn trajectory, and $\pi - |\theta_s| + \pi - |\theta_g|$ is the magnitude of the total angle turned through by the fastest turn-⇓-turn trajectory. This verifies equation 43. To complete the proof, note that any four action TCW or TCCW trajectory must turn through more than π, and costs no less in translation than the fastest three action tangent trajectory. □

Applying theorem 3 and equation 42, we immediately have the following corollary:

Corollary 1 *For every time-optimal trajectory* $\sigma(T) \leq \pi$.

Restrictions on ZR and ZL trajectories

Zigzag trajectories are composed of alternating turn or straight line actions. Successive turns or straights must be in opposite directions, but have the same magnitude. Simple geometry also gives a relationship between ϕ, the turning angle of the zigzag, and d, the length of each straight. We have:

$$d = 2b\tan(\frac{\phi}{2}) \tag{45}$$

Theorem 4 *Zigzag subsections containing three turns are not optimal.*

Proof: Consider a zigzag subsection with three turns, and two straights. The straights are the same length, so the second turn (the via point) must fall on the y axis. Construct the circle containing the start, the goal, and the via point as in Figure 4. If we perturb the via point to a nearby point on the same circle, the turning time is unchanged, and the translation is decreased. □

Zigzags can also be said to be periodic. Let τ be the smallest positive time such that:

$$\theta(t) = \theta(t + \tau)$$
$$\eta(x(t), y(t)) = \eta(x(t + \tau), y(t + \tau))$$
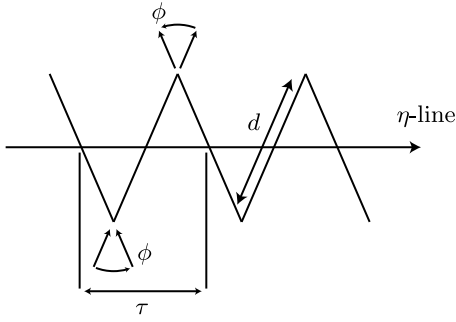
ϕ

d η-line

ϕ

τ

Figure 5: Periodicity of a zigzag

Theorem 5 *A zigzag trajectory of more than one period is not optimal.*

Proof: Consider a zigzag of more than one period, beginning at time 0 and ending at time $T > \tau$. By theorem 4, the zigzag is not optimal if $\sigma(T) > 2\phi$. If $s(T) > 2d$, then there are three straights. The first and last straights are parallel. If we reorder the segments to perform these consecutively, then we have a path which costs no more than the original but which is no longer a legitimate zigzag. Since it is not extremal, neither it nor the original path can be optimal. $\square$

Enumeration

Theorems 3, 5, and 4 allow a finite enumeration of the structure of optimal trajectories. The structure must be either one of the following, or a subsection of one of the following:

Zigzag	$\Uparrow\frown\Downarrow\frown\Uparrow$	$\Downarrow\frown\Uparrow\frown\Downarrow$	$\Uparrow\frown\Downarrow\frown\Uparrow$	$\Downarrow\frown\Uparrow\frown\Downarrow$
Tangent	$\frown\Uparrow\frown$	$\frown\Downarrow\frown$	$\frown\Uparrow\frown$	$\frown\Downarrow\frown$
Tangent	$\Uparrow\frown_\pi\Downarrow$	$\Downarrow\frown_\pi\Uparrow$	$\Uparrow\frown_\pi\Downarrow$	$\Downarrow\frown_\pi\Uparrow$

7 Summary and Conclusion.

This paper analyzed the bounded velocity differential drive model using Pontryagin's Maximum Principle. The Maximum Principle provides an elegant geometric program that generates all optimal trajectories. Further necessary conditions were used to generate a finite set of optimal trajectory structures. Our companion paper [1] analyzes this set to determine the cost and structure of the optimal trajectories between any start and goal configuration.

References

[1] D. J. Balkcom and M. T. Mason. Time optimal trajectories for bounded velocity differential drive robots. In *IEEE International Conference on Robotics and Automation*, 2000.

[2] J.-D. Boissonnat, A. Cérézo, and J. Leblond. Shortest paths of bounded curvature in the plane. In *Proceedings of the 1992 International Conference on Robotics and Automation*, pages 2315–2320, 1992.

[3] L. S. Pontryagin, V. G. Boltyanskii, R. V. Gamkrelidze, and E. F. Mishchenko. *The Mathematical Theory of Optimal Processes*. John Wiley, 1962.

[4] P. Souères and J.-D. Boissonnat. Optimal trajectories for nonholonomic mobile robots. In J.-P. Laumond, editor, *Robot Motion Planning and Control*, pages 93–170. Springer, 1998.

[5] P. Souères and J.-P. Laumond. Shortest paths synthesis for a car-like robot. *IEEE Transactions on Automatic Control*, 41(5):672–688, May 1996.

[6] H. Sussmann and G. Tang. Shortest paths for the reeds-shepp car: a worked out example of the use of geometric techniques in nonlinear optimal control. SYCON 91-10, Department of Mathematics, Rutgers University, New Brunswick, NJ 08903, 1991.